

**CALIBRATION OF THREE-DIMENSIONAL UPPER MANTLE STRUCTURE IN EURASIA
USING REGIONAL AND TELESEISMIC FULL WAVEFORM SEISMIC DATA**

Barbara Romanowicz¹, Aimin Cao¹, Ahyi Kim¹, Mark Panning², Michael E. Pasano³, and Douglas S. Dreger¹

Berkeley Seismological Laboratory¹, Princeton University², and Lawrence Livermore National Laboratory³

Sponsored by National Nuclear Security Administration
Office of Nonproliferation Research and Development
Office of Defense Nuclear Nonproliferation

Contract No. DE-FC52-04NA25543/BAA04-41

ABSTRACT

We present progress in the development of a new approach to develop and evaluate earth models at the regional scale that utilizes full waveform seismograms.

We have recently implemented a non-linear three-dimensional (3-D) Born approximation and constructed a 3-D shear velocity model of a subregion of Southeast Asia (longitude 75 to 150 degrees and latitude 0 to 45 degrees) based on this approach for the forward modeling part of the problem and linear Born kernels for the inverse part. Our initial model in the large region (longitude 30 to 150 and latitude -10 to 60 degrees) is derived from a large data set of teleseismic surface waveforms (fundamental mode and overtones in the period range 60-300 s) using the Nonlinear Asymptotic Coupling Theory (NACT), an approach used successfully for global and regional mantle tomography at Berkeley since 1995. In the subregion of study, our “N-Born” model is parameterized at relatively short wavelengths on the order of 200 km.

The NACT approach assumes two-dimensional (2-D) sensitivity kernels, confined to the vertical plane containing the source and the receiver, and is adequate for the development of a smooth velocity model. We first developed a model for Southeast Asia using NACT. Using this model as a starting model, we performed one iteration using the N-Born approach. This approach computes synthetic seismograms including the effects of single scattering (linear) as well as a non-linear part, as in the standard “path average approximation,” that accounts for large accumulated phase delays on paths that sample large scale smooth anomalies. The inversion kernels are complete 3-D Born kernels.

A regional version of the Spectral Element Method (SEM) code, RegSEM.1, has been completed. This version of the code accepts a non-conformal grid, uses PML (Perfectly Matched Layers) at the borders of the region, and includes general 3-D anisotropy, Moho and surface topography, ocean bathymetry, attenuation, and ellipticity. We are computing synthetics in our N-Born model and will perform one iteration of inversion using 3-D Born sensitivity kernels to produce the next generation 3-D model of upper mantle structure in the subregion defined above.

In order to obtain finer velocity structures beneath the region of our study, we are performing forward modeling at shorter periods using the method of frequency-wave number integration (FKI). Using our N-Born 3-D model, we add sedimentary layers in the crust and change their thickness to improve the fit to the observed seismograms, and then, based on the refined velocity structures, we conduct our own moment tensor inversions, as intermediate steps.

OBJECTIVES

The primary objective of this research is to develop and apply an approach to utilize increasingly advanced theoretical frameworks and numerical methods to obtain improved regional seismic structure calibration. Specifically, a large-scale regional Eurasian model has been developed from a large data set of seismic waveforms using the path-average approximation (PAVA) and NACT (Li and Romanowicz, 1995), which are well-developed normal-mode based approaches that consider one-dimensional (1-D) and 2-D waveform sensitivity respectively along the great-circle path between source and receiver. We refine this model in a smaller region using a linear implementation of Born single-scattering theory (Capdeville, 2005), which more accurately represents the 3-D sensitivity of the seismic wavefield, for the inverse part of the problem and using a non-linear modified 3-D Born approximation for the forward part of the problem (Panning et al., 2006). Additionally, we have developed and implemented a regional version of SEM, a numerical approach that accurately models wave propagation in a complex 3-D Earth (e.g., Faccioli et al., 1996; Komatitsch and Vilotte, 1998; Komatitsch and Tromp, 1999). Finally, we plan to utilize a novel approach with stacked sources (Capdeville et al., 2003) to further speed computation.

A further objective of this research is to perform validation and improved calibration of the model described above using a variety of approaches and data sets, including ground-truth data sets from the Knowledge Base. Specifically, we plan to apply teleseismic receiver function modeling, regional broadband data forward modeling, and surface wave group velocity measurements to test and improve the model using data not included in the original inversion. While these additional data sets can help improve all aspects of the model, we anticipate the greatest improvement in the shallow structure, particularly the crust, which is not as well constrained by the longer-period data used in the initial model development.

This research can then serve as a proof of concept for applying a similar approach to the calibration of seismic structure in other regions of Earth.

RESEARCH ACCOMPLISHED

Our NACT shear wave model (Figure 1) has been developed from a global data set of surface wave waveforms crossing the region of interest (longitude 30 to 150 degrees and latitude -10 to 60 degrees). This region is highly heterogeneous, presenting a challenge for calibration, but it is well surrounded by earthquake sources, and a significant number of high quality broadband digital stations exist. We started from the existing waveform database that was collected at Berkeley over the last 10 years for the construction of global mantle tomographic models (Li and Romanowicz, 1996; Mignan and Romanowicz, 2000; Gung et al., 2003; Panning and Romanowicz, 2004) and added data from ~20 new events in the period up to 2005. We now have 38826 3-component waveforms from 393 events recorded at 169 stations. The data has been processed using an automated algorithm, which removes glitches and checks for many common problems related to timing, poor instrument response, and excessively noisy windows. A weighting scheme has been applied to insure even distribution of data across the region. This model is parameterized laterally in spherical spline level 6, which correspond to lateral resolution of ~200 km. The corresponding radially anisotropic model is parameterized in the spline level 5, which corresponds to a lateral resolution of ~400 km.

The next step in our study has been to perform an iteration of our 3-D model using the “non-linear” Born approximation (N-Born), which is modified from the more standard 3-D “linear” Born approximation by including a “Path Average” term. This term allows the accurate inclusion of accumulated phase shifts that arise in the case when the wavepath crosses a spatially extended region with a smooth anomaly of constant sign. The linear Born terms account for single scattering effects outside of the great circle path and are modeled according to the expressions of Capdeville (2005). Accounting for scattering outside of the great-circle path is the one difference with our initial NACT approach. We demonstrate the importance of the non-linear effect in Figure 2 by comparing 3-D Born and 3-D N-Born synthetics with those of SEM. This particular case illustrates the importance of including the non-linear “path average” phase shift for paths that accumulate large phase delays.

Because the calculation of the 3-D Born sensitivity kernels is very expensive computationally, we have to select a subregion (longitude 75 to 150 degrees and latitude 0 to 45 degrees), where the lateral heterogeneities are more significant than the surrounding regions. In order to further reduce the intensity of the computation, we require that both events and stations must be in the large region (longitude 30 to 150° E and latitude -10 to 60° N) and only the ray paths along the minor arcs are selected. We calculated 3-D Born sensitivity kernels for 162 events using the

computing facilities (Jacquard) of the National Energy Research Scientific Computing Center (NERSC—www.nerc.gov). When we generate synthetics for the N-Born inversion, we use PAVA (Woodhouse and Dziewonski, 1984) in the subregion to obtain the non-linear phase term and NACT outside the subregion. The adopted damping scheme for isotropic and radially anisotropic models is the same as that used in the NACT inversion.

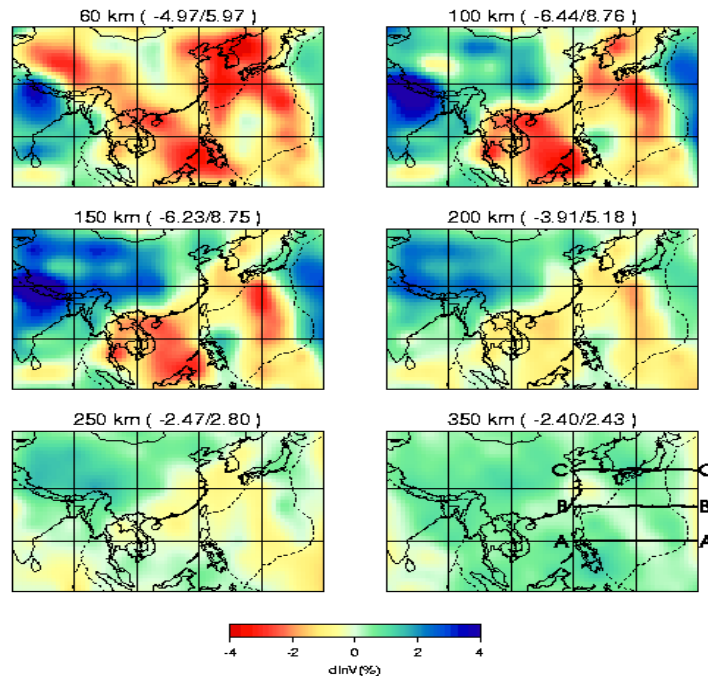


Figure 1. Starting isotropic shear velocity model derived using NACT, shown here only in the subregion (lon 75 to 150 degrees and lat 0 to 45 degrees) with map grid interval of 15 degrees. The lateral parameterization is in level 6 spherical splines, which give a resolution of ~200 km. Values are shown as percent perturbations from the isotropic velocity of the Preliminary Reference Earth Model (PREM).

Our N-Born shear velocity model is shown in Figure 3. Both N-Born and NACT derived models can fit waveforms very well, with up to ~83% variance reduction (depending on the choice of damping), and the N-Born residual variance is even lower than that of NACT (Figure 4). While the models agree in general, there are some notable differences between them in detail. For example, beneath the Tibetan plateau, the N-Born model shows a stronger fast velocity anomaly in the depth range 150 km to 250 km, which disappears at greater depth. This indicates that there is no delamination of lithosphere beneath the plateau, as has been suggested by some authors.

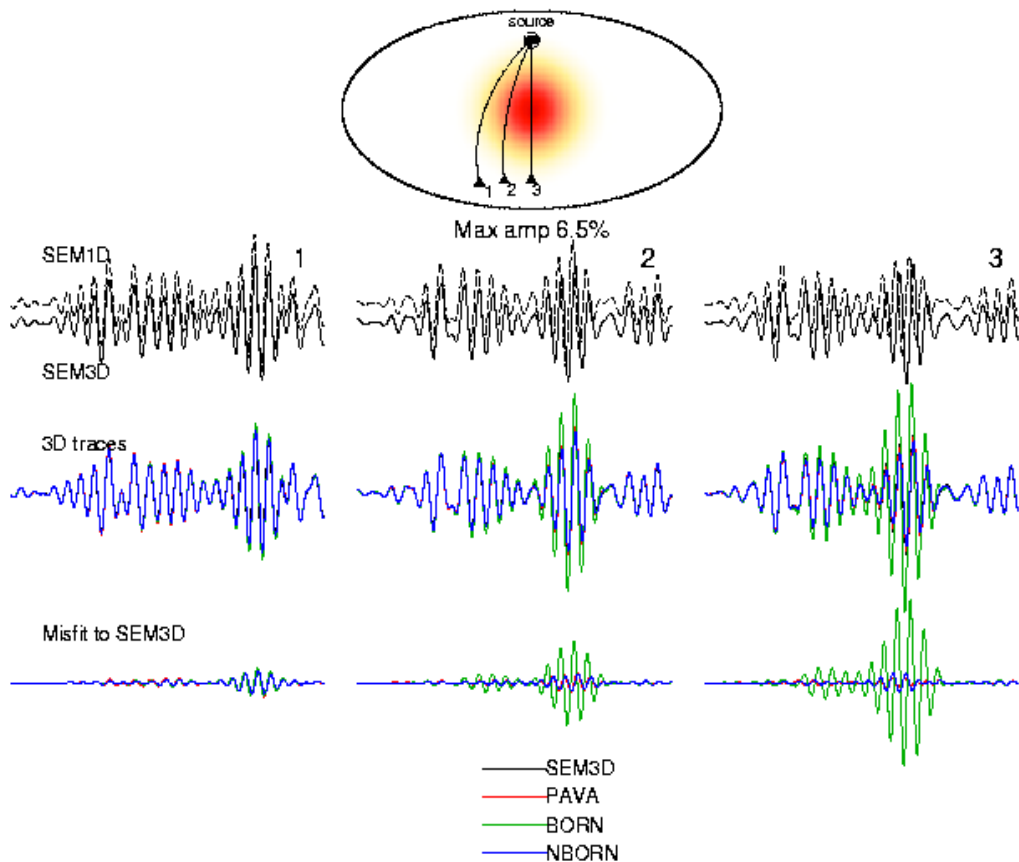


Figure 2. A comparison of synthetic seismograms using different approximations for paths through a large slow anomaly. The paths (numbered 1-3) projected on a slice of the model at 220 km depth are shown at top. The top row shows SEM synthetics through the 1-D background model (SEM1D; dashed) and through the 3-D model (SEM3D; solid) paths 1 (left), 2 (middle), and 3 (right). The middle row shows the predicted 3-D synthetics plotted on top of the SEM3D trace (black) for the path-average approximation (PAVA; red), linear Born approximation (BORN; green), and non-linearly modified Born (NBORN; blue). The bottom row shows the misfits for PAVA, BORN, and NBORN to the SEM3D trace. The amplitude is scaled to the maximum of the SEM3D trace in each column. While the Born approach is important to represent the 3-D effects in many configurations, this figure illustrates the case of a path sampling the center of a large anomaly. In this case, the non-linear, path average contribution to the seismogram dominates, and the linear Born approximation does a poor job at predicting the waveforms.

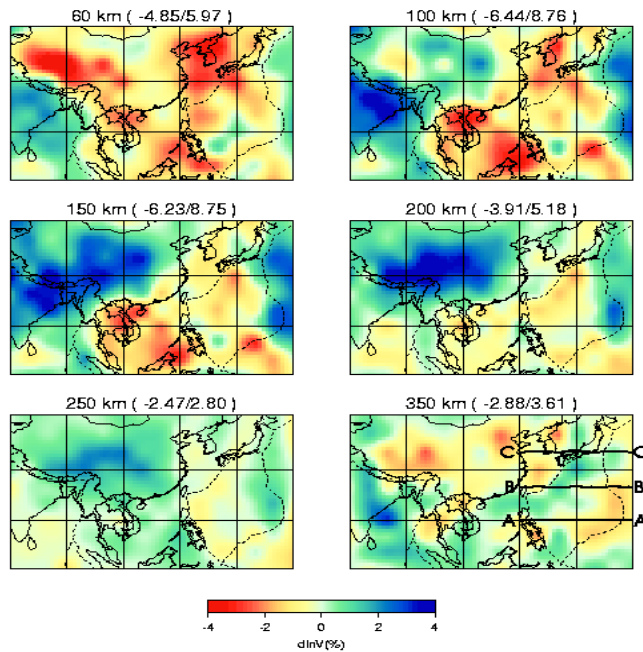


Figure 3. N-Born isotropic shear velocity model derived using the “non-linear” 3-D Born approximation in the same subregion as in Figure 1.

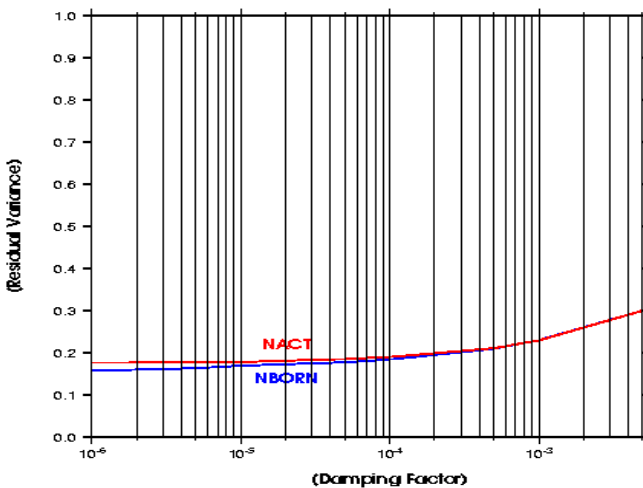


Figure 4. Residual variance as a function of the damping factor. In both N-Born and NACT models, the chosen damping factor for the models shown respectively in Figure 3 and Figure 1 is 5.0E-5.

In collaboration with researchers at Institut de Physique du Globe de Paris (IPGP), we have completed a regional version of the Spectral Element code (RegSEM.1). The regional SEM incorporates PML boundary conditions on the lateral borders of the region, which effectively eliminate spurious reflections from the borders, and a non-conforming mesh. Compared with previous versions, first of all, both Moho topography and surface topography have been included into the process of building the mesh. With reference to a Moho model, every element in the simulation domain is assigned an integer (1 for elements just above the Moho, -1 for those just below, and 0 for the others), and we are able to provide realistic velocity contrasts at the Moho discontinuity while introducing any 3-D elastic mantle model. Second, anisotropy has been included in this new version of regional SEM (any anisotropic structure can be considered). Third, we do not need to rotate events, stations, and models to be centered at the North

Pole before the simulation, as required in the previous versions. All the rotations can be done automatically, and all the input information related to the event focal mechanism and station coordinates are straightforward. Thus, it is now very convenient to add more stations into the station list. Finally, this new version of regional SEM has been fully optimized. The same computation now takes only one-third of the previous cluster hours. This will be very helpful for our future waveform inversion using the regional SEM method. For demonstration, we examine the effect of the Moho topography (CRUST2.0) on the synthetic waveforms computed in our NACT velocity model (Figure 5). Inclusion of the Moho topography can significantly change the fundamental Rayleigh waveforms in not only travel time but also amplitude. For the ray paths with significant oceanic portion (DAV), the shape of the waveform is also changed (Figure 6).

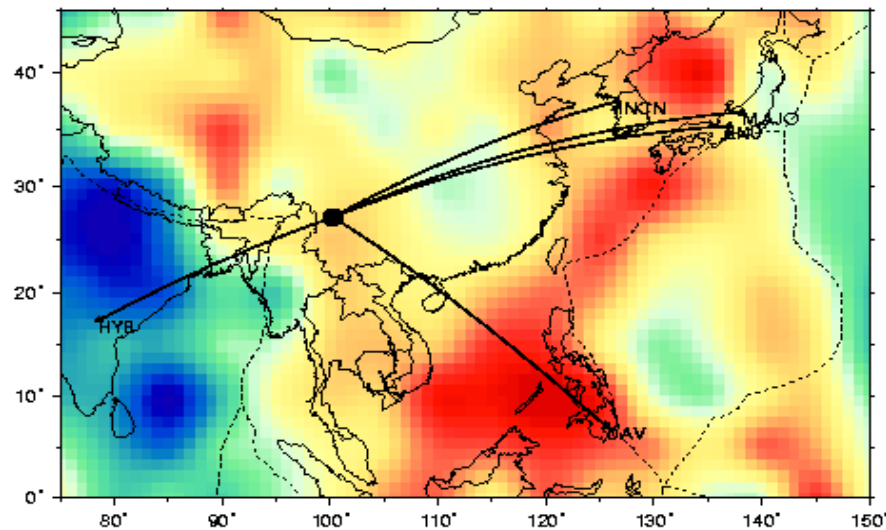


Figure 5. Map showing event and station locations for the SEM simulation shown in Figure 6. The background is our most recent model derived using NACT, shown at a depth of 60 km.

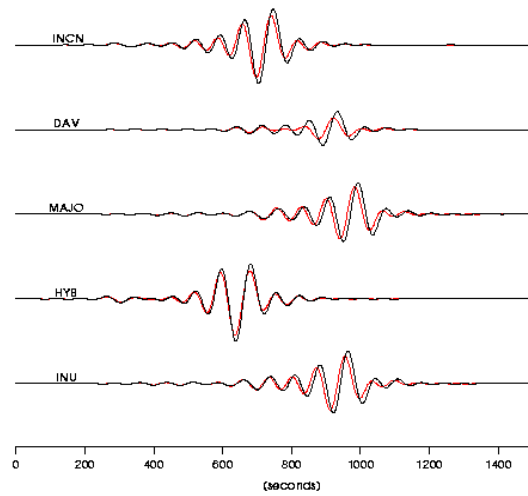


Figure 6. Comparison of vertical component SEM synthetics in our NACT derived model (Figure 1) with (red) and without (black) consideration of the Moho topography. Synthetics have been low-pass filtered with a corner at 60 sec.

In order to refine the velocity structure beneath the region of our study, we perform forward waveform modeling with the FKI method. Broadband seismograms are downloaded from the Incorporated Research Institutions for Seismology (IRIS) and corrected to absolute ground velocity (cm/sec). We show 2 event locations of events 2000256 (9/12/2000, Mw6.1) and 2003107 (4/17/2003, Mw6.3) and the IRIS station distributions (Figure 7). We start with the 2000256 event, for which the continental ray paths are dominant, to obtain the 1-D velocity structure between the source and each receiver. Broadband data are bandpass filtered at 0.005-0.05 Hz. We used the Harvard centroid moment tensor (CMT) solution for the source parameters, and the starting model is a 1-D layered average crustal velocity structure derived from CRUST2.0. Using the best velocity model we can obtain (Figure 8), we compute Green's functions and perform the moment tensor analysis for two ranges of frequency (0.01-0.05 Hz and 0.005-0.03 Hz). Then, we select the event 2003107, for which we have ray paths similar to event 2000256, to perform the moment tensor analysis using Green's function obtained from our 1-D simulation (Figure 9). We find a moment tensor solution in good agreement with the CMT solution, whereas the solution obtained using the PREM reference model is very poor. While this example was chosen because we expect that we can use Harvard CMT solutions for M>6 events as good references, this indicates that the additional regional modeling effort is worthwhile and will lead to better moment tensor solutions for smaller events in the area, when we extend the modeling to higher frequencies (0.02-0.05 Hz).

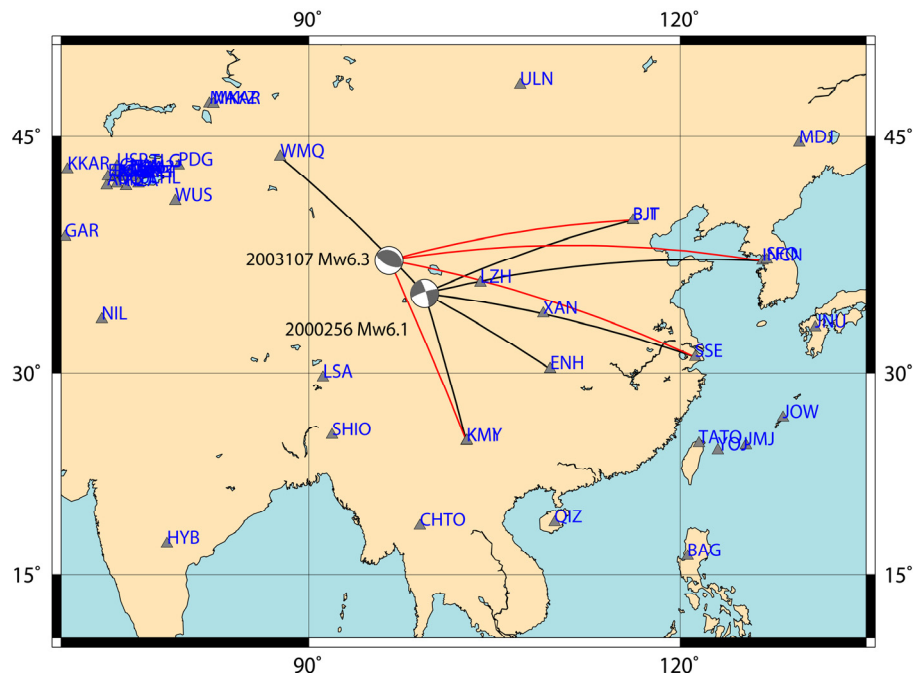


Figure 7. Event 2000256 (9/12/2000, Mw6.1), 2003107 (4/17/2003, Mw6.3), and IRIS station distributions. Source 2000256 (9/12/2000, Mw6.1) is used to obtain the velocity structures.

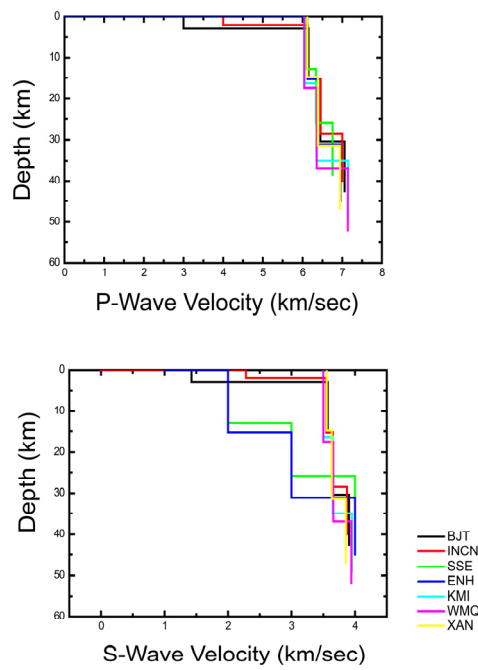


Figure 8. Best P-wave and S-wave velocity structures for the paths between event 2000256 and IRIS stations obtained from 1-D forward modeling.

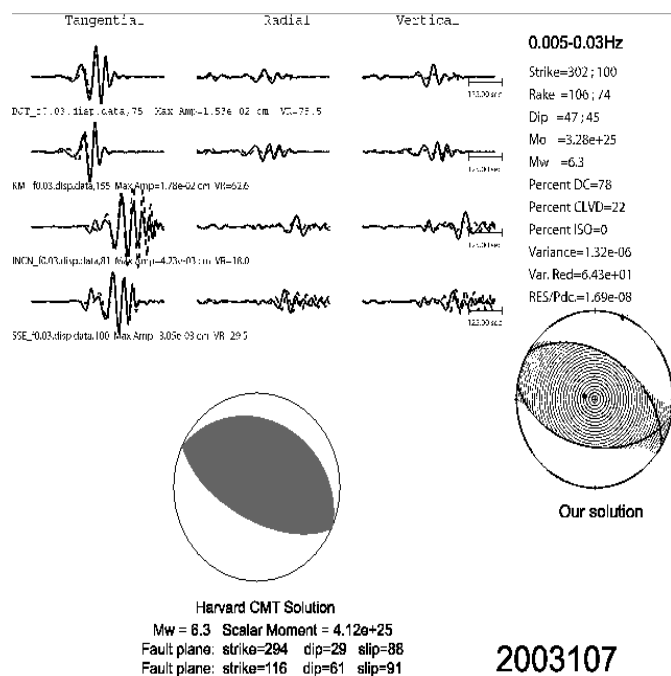


Figure 9. Top: Moment tensor solution for event 2003107 in the 0.005-0.03 Hz range using Green's function computed from the velocity model obtained using the 2000256 event (Figure 9). Bottom: Global CMT solution from Harvard University.

CONCLUSIONS AND RECOMMENDATIONS

A 3-D non-Linear Born implementation is shown to be promising to accurately model large scale lateral structures. This approach includes relatively rapid calculation of partial derivatives for use in the next inversion step where the forward modeling will be performed using the recently completed regional SEM numerical code.

Further work on the regional SEM synthetics and 3-D Born sensitivity kernels should offer continued improvement of the model. We are in the process of implementing an iteration of our model using the regional SEM code. Additionally, other approaches and data sets, including ground-truth data sets from the Knowledge Base, teleseismic receiver functions, broadband waveform forward modeling at shorter periods, and surface wave group velocities will allow for validation and improvement of the model and, in particular, for improved moment tensor solutions.

ACKNOWLEDGEMENTS

We would like to acknowledge the contributions of Yann Capdeville and Paul Cupillard at IPGP, who did extensive work on both the Born and SEM codes. Many computations were performed using computing resources obtained through a time allocation at NERSC from the Department of Energy (DOE) Office of Science, Geosciences Division, for which we thank Dr. Nick Woodward of DOE.

REFERENCES

- Capdeville, Y., B. Romanowicz, and Y. Gung (2003). Global seismic waveform tomography based on the spectral element method, abstract, joint AGU/EGS/EUG Meeting, Nice, April 2003.
- Capdeville, Y. (2005). An efficient Born normal mode method to compute sensitivity kernels and synthetic seismograms in the Earth, *Geophys. J. Int.* 163: 639–646.
- Faccioli, E., F. Maggio, A. Quarteroni, and A. Tagliani (1996). Spectral-domain decomposition methods for the solution of acoustic and elastic wave equations, *Geophysics* 61: 1160–1174.
- Gung, Y., B. Romanowicz, and M. Panning (2003). Anisotropy and lithospheric thickness, *Nature* 422: 707–711.
- Komatitsch, D. and J. P. Vilotte (1998). The spectral element method: an effective tool to simulate the seismic response of 2D and 3D geological structures, *Bull. Seism. Soc. Am.* 88: 368–392.
- Komatitsch, D. and J. Tromp (1999). Introduction to the spectral-element method for 3-D seismic wave propagation, *Geophys. J. Int.* 139: 806–822.
- Li, X. D. and B. Romanowicz (1995). Comparison of global waveform inversions with and without considering cross branch coupling, *Geophys. J. Int.* 121: 695–709.
- Li, X. D. and B. Romanowicz (1996). Global mantle shear velocity model developed using nonlinear asymptotic coupling theory, *J. Geophys. Res.* 101: 22,245–22,273.
- Megnin, C. and B. Romanowicz (2000). The 3D shear velocity structure of the mantle from the inversion of body, surface and higher mode waveforms, *Geophys. J. Int.* 143: 709–728.
- Panning, M. and B. Romanowicz (2004). Inferences on flow at the base of Earth's mantle based on seismic anisotropy, *Science* 303: 351–353.
- Panning, M., F. Marone, A. Kim, Y. Capdeville, P. Cupillard, Y. Gung, and B. Romanowicz (2006). Improvements in mode-based waveform modeling and application to Eurasian velocity structure, *Eos. Trans. AGU*, 87(52). Fall Meet. Suppl.
- Woodhouse, J.H. and A.M. Dziewonski (1984). Mapping the upper mantle: Three dimensional modeling of Earth's structure by inversion of seismic waveforms, *J. Geophys. Res.* 89: 5953–5986.